

Mechanistic studies on monodentate–ligand substitution of five-coordinate trigonal-bipyramidal platinum (II) complexes with tris[2-(diphenylphosphino)ethyl]phosphine

Sen-ichi Aizawa^{a,*}, Tadashi Kobayashi^a, Tatsuya Kawamoto^b

^a Faculty of Engineering, Toyama University, 3190 Gofuku, Toyama 930-8555, Japan

^b Department of Chemistry, Graduate School of Science, Osaka University, 1-16 Machikaneyama, Toyonaka, Osaka 560-0043, Japan

Received 30 October 2004; accepted 24 November 2004

Abstract

Reaction of the five-coordinate trigonal-bipyramidal platinum(II) complex, $[\text{Pt}(\text{pt})(\text{pp}_3)](\text{BF}_4)$ (pt = 1-propanethiolate, pp_3 = tris[2-(diphenylphosphino)ethyl]phosphine), with I^- in chloroform gave the five-coordinate square-pyramidal complex with a dissociated terminal phosphino group and an apically coordinated iodide ion in equilibrium. The thermodynamic parameters for the equilibrium between the trigonal-bipyramidal and square-pyramidal geometries, $[\text{Pt}(\text{pt})(\text{pp}_3)]^+ + \text{I}^- \rightleftharpoons [\text{PtI}(\text{pt})(\text{pp}_3)]$, and the kinetic parameters for the chemical exchange were obtained as follows: $K_{\text{ex}}^{298} = 7.5 \times 10^{-1} \text{ mol}^{-1} \text{ kg}$, $\Delta H^0 = -10 \pm 2.4 \text{ kJ mol}^{-1}$, $\Delta S^0 = -36 \pm 10 \text{ J K}^{-1} \text{ mol}^{-1}$, $k_{\text{ex}}^{298} = 1.3 \times 10^4 \text{ s}^{-1}$, $\Delta H^\ddagger = 34 \pm 4.7 \text{ kJ mol}^{-1}$, $\Delta S^\ddagger = -50 \pm 21 \text{ J K}^{-1} \text{ mol}^{-1}$. The square-planar trinuclear platinum(II) complex was formed by bridging reaction of one of the terminal phosphino groups of trigonal-bipyramidal $[\text{PtCl}(\text{pp}_3)]\text{Cl}$ with *trans*- $[\text{PtCl}_2(\text{NCC}_6\text{H}_5)_2]$ in chloroform. From these facts, ligand substitution reactions of $[\text{PtX}(\text{pp}_3)]^+$ (X = monodentate anion) are expected to proceed via an intermediate with a dissociated phosphino group. The rate constants for the chloro-ligand substitution reactions of $[\text{PtCl}(\text{pp}_3)]^+$ with Br^- and I^- in chloroform approached the respective limiting values as concentrations of the entering halide ions are increased. These kinetic results confirmed the preassociation mechanism in which the square pyramidal intermediate with a dissociated phosphino group and an apically coordinated halide ion is present in the rapid pre-equilibrium.

© 2005 Elsevier B.V. All rights reserved.

Keywords: Trigonal-bipyramidal platinum(II) complex; Trigonal-bipyramidal–square-pyramidal equilibrium; Preassociation mechanism

1. Introduction

Reaction mechanisms of four-coordinate square-planar palladium(II) and platinum(II) complexes have been well investigated so far, and the associative mechanism via a trigonal-bipyramidal 18-electron transition state has been generally proposed [1]. On the other hand, kinetic properties of five-coordinate trigonal-bipyramidal palladium(II) or platinum(II) complexes with an 18-electron ground state have not been sufficiently investigated and the general reaction mechanism is still unclear. Re-

cently, we have carried out a few kinetic studies on ligand substitution reactions of some trigonal-bipyramidal palladium(II) complexes with tris[2-(diphenylphosphino)ethyl]phosphine (pp_3) as a bound ligand [2,3], because the pp_3 ligand tends to form the stable trigonal-bipyramidal complexes with d^8 metal ions [4,5]. In the case of the substitution reactions of $[\text{PdX}(\text{pp}_3)]\text{X}$ ($\text{X} = \text{Cl}, \text{Br}, \text{I}$) with trimethyl phosphite in chloroform, the observed rate constants were proportional to the concentration of entering trimethyl phosphite and the associative mechanism was expected from the obtained activation parameters [2]. In contrast to the reaction of the haro complexes with neutral phosphite, the rate constants for the reaction of the thiolato complexes

* Corresponding author. Tel./fax: +81 76 445 6980.

E-mail address: saizawa@eng.toyama-u.ac.jp (S. Aizawa).

[Pd(SR)(pp₃)](BF₄) (SR = 1-propanethiolate, α -toluenethiolate) with halide ions in chloroform were independent of concentration of the entering halide ions, which was tentatively attributed to the ion-pair formation of the positively charged thiolato complexes with halide anions in the weakly polar solvent [3]. Furthermore, the reactions showed rather dissociative character the degree of which depends largely on the entering halide ions. On the assumption that the attack of negatively charged halide ions onto the palladium(II) center with the electron-donating thiolato ligand brings about greater electronic repulsion than that of relatively electron-accepting phosphite onto the haro complexes, the variation in the reaction mechanism can be explained by difference in the electronic repulsion in the transition state. However, the argument may not be necessarily convincing considering a possibility that an undetectable intermediate is present in rapid pre-equilibrium. Accordingly, we have pursued further investigation by using the corresponding platinum(II) complexes because the intermediates or unstable species might be detectable due to the greater activation energy for each elementary reaction.

In this work, we have disclosed the pre-equilibrium and the intermediate for the substitution reactions of the trigonal-bipyramidal platinum(II) complexes with the pp₃ ligand by investigating the reactions of [Pt(pt)-(pp₃)](BF₄) (pt = 1-propanethiolate) and [PtCl(pp₃)]Cl with halide ions in completely dry conditions. These results can also provide us further insight into the kinetic properties of the trigonal-bipyramidal palladium (II) complexes.

2. Experimental

2.1. Reagents

Chloroform (Wako, ∞ pure) and deuterated chloroform (CDCl₃, Aldrich) were dried over activated 4A Molecular Sieves. Tris[2-(diphenylphosphino)ethyl] phosphine (pp₃, Aldrich), potassium tetrachloroplatinate(II) (Wako), tetra-*n*-butylammonium bromide and iodide (*n*-Bu₄NBr and *n*-Bu₄NI), 1-propanethiol (Hpt, Wako) and dichlorobis(benzonitrile)platinum(II) (Strem) were used for preparation without further purification.

2.2. Preparation of complexes

2.2.1. [PtCl(pp₃)]Cl (1)

Complex **1**·H₂O was prepared by a similar procedure described in the literature [5]. Yield 98%. *Anal.* Calc. for C₄₂H₄₂P₄Cl₂Pt·H₂O: C, 51.38; H, 4.31; N, 0.00. Found: C, 51.37; H, 4.53; N, 0.00%. ³¹P{¹H} NMR(CHCl₃): σ 26.8 (s, 3P, terminal, ¹J_{P-Pt} = 2588 Hz), 120.1 (s, 1P, cen-

ter, ¹J_{P-Pt} = 2506 Hz). UV-vis (in CHCl₃): λ_{\max} /nm (log(ϵ /mol⁻¹ kg cm⁻¹)) 417 (3.81), 369 (3.91). Complex **1**·H₂O was recrystallized from a mixture of acetonitrile and chloroform to remove the crystallizing water. Single crystals of **1**·CH₃CN were obtained¹ and it was confirmed by the ¹H NMR measurements that the crystallizing acetonitrile is volatile in vacuo.

2.2.2. [PtBr(pp₃)]Br (2)

To a solution of **1**·H₂O (0.11 g, 0.12 mmol) in chloroform (10 cm³) was added excess *n*-Bu₄NBr (0.24 g, 0.74 mmol). The solution was stirred for 1 h at room temperature and then concentrated gradually to a small volume. The resultant yellow crystals were collected by filtration and air-dried. Yield: 88%. *Anal.* Calc. for C₄₂H₄₂P₄Br₂Pt·2H₂O: C, 47.52; H, 4.37; N, 0.00. Found: C, 47.32; H, 4.46; N, 0.00%. ³¹P{¹H} NMR (CHCl₃): σ 23.6 (s, 3P, terminal, ¹J_{P-Pt} = 2575 Hz), 124.7 (s, 1P, center, ¹J_{P-Pt} = 2491 Hz). UV-vis (in CHCl₃): λ_{\max} /nm (log(ϵ /mol⁻¹ kg cm⁻¹)) 427 (3.86), 380 (3.91).

2.2.3. [PtI(pp₃)]I (3)

The iodo complex (**3**) was prepared by the haro-ligand substitution reaction similar to that for the bromo complex (**2**) using 0.22 g (0.24 mmol) of **1**·H₂O and excess *n*-Bu₄NI (0.37, 1.00 mmol) instead of *n*-Bu₄NBr. Yield: 84%. *Anal.* Calc. for C₄₂H₄₂P₄I₂Pt·H₂O: C, 44.34; H, 3.90; N, 0.00. Found: C, 44.50; H, 3.73; N, 0.00%. ³¹P{¹H} NMR (CHCl₃): σ 18.5 (s, 3P, terminal, ¹J_{P-Pt} = 2572 Hz), 129.4 (s, 1P, center, ¹J_{P-Pt} = 2395 Hz). UV-vis (in CHCl₃): λ_{\max} /nm (log(ϵ /mol⁻¹ kg cm⁻¹)) 441 (3.89), 409 (3.92).

2.2.4. [Pt(pt)(pp₃)](BF₄) (4)

To a solution of **1**·H₂O (0.51 g, 0.54 mmol) in chloroform (50 cm³) was added AgBF₄ (0.23 g, 1.18 mmol). After removal of precipitated AgCl by filtration, to the colorless filtrate was added a solution of 1-propanethiol (Hpt, 0.045 g, 0.54 mmol) in chloroform (5 cm³), and then a 0.5 M NaOH aqueous solution (10 cm³), water (5 cm³) and ethanol (30 cm³). The mixture was stirred for 5 min at room temperature and NaOH was extracted with several 150 cm³ portions of water. Finally, to the separated chloroform layer was added ethanol and water gradually. The resultant yellow needle crystals were collected by filtration and air-dried. Yield: 60%. *Anal.* Calc. for C₄₅H₄₉BF₄P₄SPT·H₂O: C, 51.68; H, 4.92; N, 0.00. Found: C, 51.69; H, 4.70; N, 0.00%. ³¹P{¹H} NMR (CHCl₃): σ 20.2 (s, 3P, terminal,

¹ The X-ray diffraction measurements were carried out using the crystal sealed in a Lindemann glass-capillary tube with the mother liquor. Because the crystal structure of **1**·6H₂O was reported recently in [5], our crystallographic data for **1**·CH₃CN were merely deposited as a supplementary material.

$^1J_{\text{P-Pt}} = 2650$ Hz), 126.3 (s, 1P, center, $^1J_{\text{P-Pt}} = 1940$ Hz). UV–vis (in CHCl_3): $\lambda_{\text{max}}/\text{nm}$ ($\log(\epsilon/\text{mol}^{-1} \text{ kg cm}^{-1})$) 449 (3.95), 360 (3.52 sh).

2.2.5. $[\text{Pt}_3\text{Cl}_4(\text{pp}_3)_2]\text{Cl}_2$ (5)

The Pt(II) trinuclear complex was prepared by bridging reaction of the five-coordinate trigonal-bipyramidal Pt(II) complex $\mathbf{1} \cdot \text{H}_2\text{O}$ (0.32 g, 0.34 mmol) with *trans*- $[\text{PtCl}_2(\text{NCC}_6\text{H}_5)_2]$ (0.080 g, 0.17 mmol) as a metal complex to be bridged in chloroform. The reaction solution was allowed to stand at room temperature for 2 days and to this was added diethylether to give pale yellow crystals. Yield: 79%. Anal. Calc. for $\text{C}_{84}\text{H}_{84}\text{P}_8\text{Cl}_6\text{Pt}_3 \cdot 2\text{H}_2\text{O}$: C, 46.38; H, 4.08; N, 0.00. Found: C, 45.91; H, 4.04; N, 0.00%. $^{31}\text{P}\{^1\text{H}\}$ NMR (CHCl_3): σ 11.4 (m, 2P, terminal, $^1J_{\text{P-Pt}} = 3670$ Hz, $^2J_{\text{P-P}} = 15.5$ Hz, $^3J_{\text{P-P}} = 48.0$ Hz), 42.0 (s, 4P, terminal, $^1J_{\text{P-Pt}} = 2492$ Hz), 88.2 (m, 2P, center, $^1J_{\text{P-Pt}} = 2925$ Hz). $^{195}\text{Pt}\{^1\text{H}\}$ NMR (CHCl_3): σ 285.3 (t, 1Pt, center, $^1J_{\text{Pt-P}} = 3675$ Hz), -99.8 (dt, 2Pt, terminal, $^1J_{\text{Pt-P(terminal)}} = 2920$ Hz, $^1J_{\text{Pt-P(center)}} = 2494$ Hz).

2.3. Measurements

Sample preparations for kinetics of $\mathbf{1}$ were carried out under a nitrogen atmosphere using completely dried chloroform, *n*- Bu_4NX ($\text{X}^- = \text{Br}^-, \text{I}^-$) and $\mathbf{1}$ obtained from $\mathbf{1} \cdot \text{CH}_3\text{CN}$ in vacuo. The kinetic measurements were performed at 298 K under pseudo-first-order conditions where the concentrations of X^- (2.5×10^{-2} – $2.5 \times 10^{-1} \text{ mol kg}^{-1}$) were in large excess over that of $\mathbf{1}$ ($7.8 \times 10^{-5} \text{ mol kg}^{-1}$). The temperature of the reaction solutions was controlled within ± 0.1 K. The absorption spectral changes were recorded on a Perkin–Elmer Lambda 19 spectrophotometer.

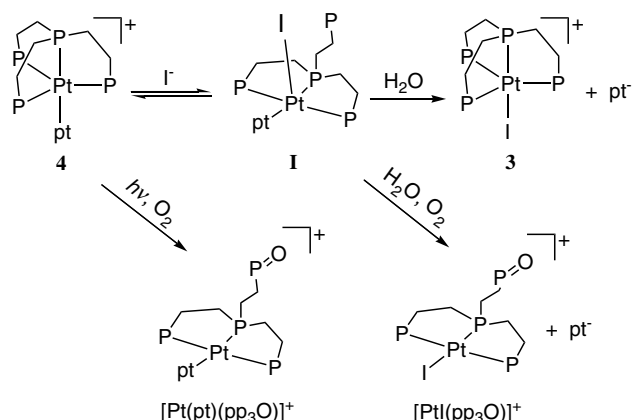
^{195}Pt , ^{31}P and ^1H NMR spectra were recorded on a JEOL JNM-A400 FT-NMR spectrometer operating at 85.48, 160.70 and 399.65 MHz, respectively. In order to determine the chemical shifts of ^{195}Pt and ^{31}P NMR signals, a 3 mm o.d. NMR tube containing the sample solution was coaxially mounted in a 5 mm o.d. NMR tube containing deuterated water as a lock solvent and $\text{K}_2[\text{Pt}(\text{CN})_4]$ and phosphoric acid as references, respectively. NMR samples for equilibrium and kinetic experiments for $\mathbf{4}$ were prepared by vacuum distillation of dried CDCl_3 into NMR tubes containing the completely dried sample that were then flame-sealed after degassing. The equilibrium constants were evaluated from initial concentrations of $\mathbf{4}$ and *n*- Bu_4NI and relative intensities of the non-decoupled ^{31}P NMR signals for the equilibrated species obtained by taking a sufficiently long acquisition time in the temperature range from 206.5 to 236.7 K. The chemical exchange rate constants were given by increase in transverse relaxation rates obtained from the spectral simulation of the line-broadening data in the temperature range from 219.5 to 234.9 K. The

temperatures of the NMR sample solutions were determined by direct measurements of the solvent temperature in an NMR tube set in the probe using a Technol Seven D617 digital thermister and were controlled within ± 0.1 K.

3. Results and discussion

3.1. Rapid equilibrium

The ^{31}P NMR spectra of $\mathbf{1}$ – $\mathbf{4}$ in chloroform indicate the trigonal-bipyramidal structure with C_3 symmetry exhibiting two signals coupled with ^{195}Pt which are assigned to the three equivalent terminal phosphorus atoms of the pp_3 ligand in the equatorial position and the central phosphorus atom in the axial position. The coupling between the Pt(II) ion and the axial phosphorus atom of the pt complex $\mathbf{4}$ ($^1J_{\text{P-Pt}} = 1940$ Hz) is definitely weak compared with those of the haro complexes $\mathbf{1}$ – $\mathbf{3}$ ($^1J_{\text{P-Pt}} = 2506$ – 2395 Hz) due to the strong trans inference of the thiolato sulfur atom. The electronic absorption spectra of $\mathbf{1}$ – $\mathbf{4}$ in chloroform are also consistent with the five-coordinate trigonal-bipyramidal geometry showing two d–d absorption bands in the visible or near UV regions assigned to the transitions from $^1\text{A}'_1$ to $^1\text{E}'$ and $^1\text{E}''$ (see Section 2) [6]. The ^{31}P NMR spectrum of $\mathbf{4}$ in chloroform was gradually changed under a luminescent lamp to give quantitatively the square-planar complex with a dissociated phosphine oxide group, $[\text{Pt}(\text{pt})(\text{pp}_3\text{O})]^+$ (Scheme 1), exhibiting ^{31}P NMR signals at 32.3 ppm (phosphine oxide, $^3J_{\text{P-P}} = 37$ Hz), 44.6 ppm (terminal, $^1J_{\text{P-Pt}} = 2648$ Hz) and 91.7 ppm (center, $^1J_{\text{P-Pt}} = 2122$ Hz) (Fig. S1, Supplementary material), while the oxidation reaction hardly proceeded in the dark or in the deoxygenated solution. The substitution reaction of $\mathbf{4}$ with I^- proceeded in an unsealed chloroform solution to give the iodo complex $\mathbf{3}$ and the square-planar iodo complex with a dissociated



Scheme 1. Substitution and oxidation reactions of $\mathbf{4}$ in chloroform.

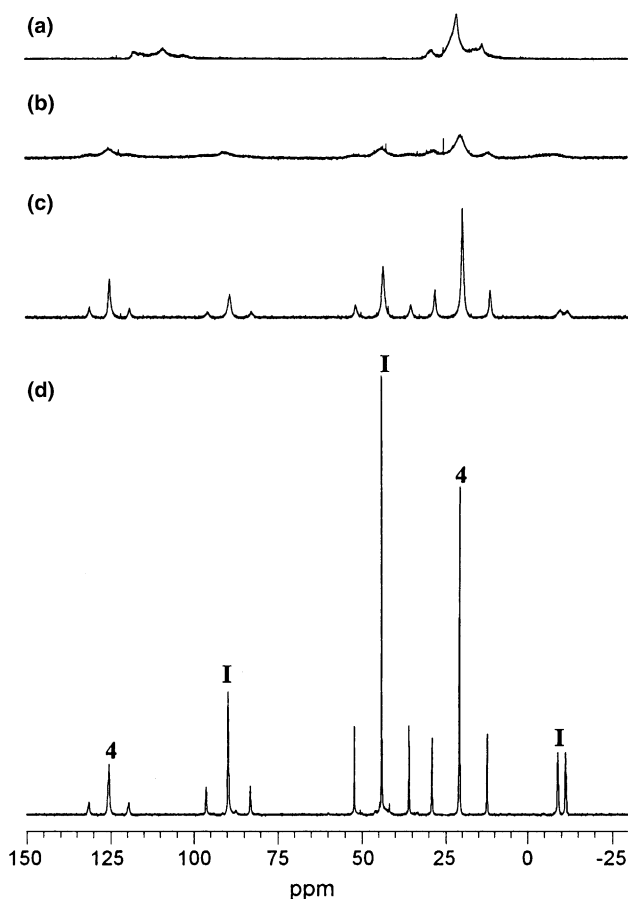


Fig. 1. ^{31}P NMR spectra of CDCl_3 solution of **4** ($2.2 \times 10^{-2} \text{ mol kg}^{-1}$) containing a large excess of NBu_4I ($4.1 \times 10^{-1} \text{ mol kg}^{-1}$) at 298.3 (a), 250.0 (b), 236.9 (c) and 206.7 (d) K. **4s** and **I**s denote the signals for the corresponding complexes.

phosphine oxide group, $[\text{PtI}(\text{pp}_3\text{O})]^+$ (Scheme 1), exhibiting ^{31}P NMR signals at 32.2 ppm (phosphine oxide, $^3J_{\text{P-P}} = 37 \text{ Hz}$), 42.2 ppm (terminal, $^1J_{\text{P-Pt}} = 2434 \text{ Hz}$), and 95.0 ppm (center, $^1J_{\text{P-Pt}} = 2800 \text{ Hz}$) (Fig. S2, Supplementary material). On the other hand, the sealed sample solution containing **4** and a large excess of $n\text{-Bu}_4\text{NI}$ in completely deoxygenated and dried CDCl_3 showed extremely broad ^{31}P NMR signals at room temperature, which were sharpened as the temperature was lowered (Fig. 1). Three sets of signals other than the signals of **4** were clearly observed at the lower temperature and the spectrum was changed reversibly with temperature. By comparison with the ^{31}P NMR spectra of square-planar $[\text{Pt}(\text{pt})(\text{pp}_3\text{O})](\text{BF}_4)$ (see above) and the free pp_3 ligand², the two signals at 44.0 and 89.6 ppm coupled with ^{195}Pt ($J_{\text{P-Pt}} = 2644$ and 2116 Hz , respectively) are assigned to the two terminal and central phosphorus atoms on the Pt(II) square-plane, respectively, and a pair of signals at -9.1 and -11.4 ppm corre-

² $^{31}\text{P}\{^1\text{H}\}$ NMR (CHCl_3): $\sigma -13.0$ (d, 3P, terminal), -17.5 (q, 1P, center); $^3J_{\text{P-P}} = 26 \text{ Hz}$.

sponds to the free terminal phosphorus atom. Considering that the relative strength of these signals increases with an increase of the I^- concentration, the above finding is attributable to formation of the square-pyramidal Pt(II) complex with a dissociated terminal phosphino group and an apically coordinated I^- (**I** in Scheme 1). Coordination of the pt ligand in the square-plane is confirmed by the chemical shifts and the $J_{\text{P-Pt}}$ values for the coordinated terminal and central phosphorus atoms of **I** that are in good agreement with those of $[\text{Pt}(\text{pt})(\text{pp}_3\text{O})]^+$ but entirely different from those of $[\text{PtI}(\text{pp}_3\text{O})]^+$. Because the two isomeric structures, one with the iodo ligand and the pendant diphenylphosphinoethyl group on the same side of the Pt(II) square plane and the other on the opposite side, are possible for **I**, we can assume that the two relatively broad resonance lines observed in the region of the free diphenylphosphino group at the lower temperature are due to the two different steric surroundings.

By addition of a small amount of water to the equilibrated solution, the substitution reaction of the pt ligand with I^- proceeded to give the five-coordinate trigonal-bipyramidal iodo complex **3** (Scheme 1). This fact indicates that re-coordination of the free terminal phosphino group accompanies release of the pt ligand bound to Pt(II) into the moist chloroform because of the greater solvation energy for pt^- compared with dry chloroform. Formation of $[\text{PtI}(\text{pp}_3\text{O})]^+$ in the unsealed solution in the dark indicates that the dissociated terminal phosphino group in **I** is partially oxidized in the course of the pt ligand substitution reaction with I^- (Scheme 1). The equilibrium constant at 298 K and the enthalpy and entropy changes for the formation of **I** in CDCl_3 were obtained by using the change in ratio of the ^{31}P NMR intensity with temperature at which the ^{31}P NMR signals for **4** and **I** are well resolved (see Section 2) as follows: $K_{\text{ex}}^{298} = 7.5 \times 10^{-1} \text{ mol}^{-1} \text{ kg}$, $\Delta H^0 = -10 \pm 2.4 \text{ kJ mol}^{-1}$,

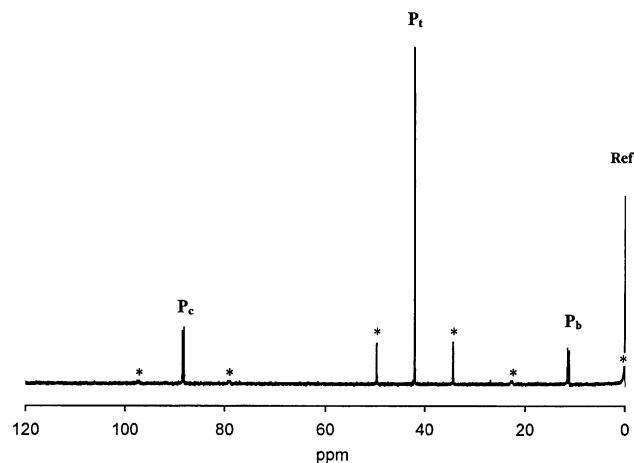


Fig. 2. ^{31}P NMR spectra of **5** in CHCl_3 . P_c , P_t and P_b are assigned to the signals for the central, terminal and bridging phosphorus atoms, respectively. Asterisks and 'ref' denote satellite peaks due to ^{195}Pt and the signal for D_3PO_4 in the outer D_2O , respectively.

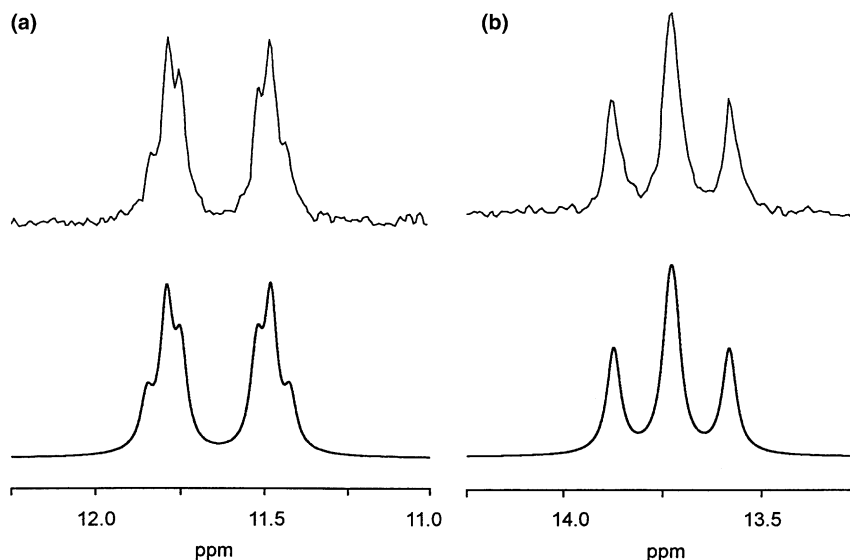


Fig. 3. Observed (upper) and simulated (lower) ^{31}P NMR spectra for the bridging phosphorus atoms of **5** (a) and the intermediate (b). The simulated spectra are depicted by using $^2J_{\text{P-P}}=15$ Hz and $^3J_{\text{P-P}}=48$ Hz for **5** and $^2J_{\text{P-P}}=490$ Hz and $^3J_{\text{P-P}}=48$ Hz for the intermediate.

$\Delta S^0 = -36 \pm 10 \text{ J K}^{-1} \text{ mol}^{-1}$ (Fig. S3, Supplementary material). These thermodynamic parameters reveal that **I** is enthalpically a little stable but entropically unstable compared with **4** due to coordination of free I^- . The observed chemical exchange rate constant at 298 K and the activation enthalpy and entropy were estimated to be $1.3 \times 10^4 \text{ s}^{-1}$, $34 \pm 4.7 \text{ kJ mol}^{-1}$ and $-50 \pm 21 \text{ J K}^{-1} \text{ mol}^{-1}$, respectively, by using the ^{31}P NMR line-broadening data of **4** under the same conditions described in Fig. 1 (Fig. S4, Supplementary material). This exchange rate is extremely faster than the usual substitution rates for square-planar Pt(II) complexes [7].

3.2. Bridging reaction

The complex **5** obtained by the reaction of *trans*- $[\text{PtCl}_2(\text{NCC}_6\text{H}_5)_2]$ with 2 equiv of **1** in chloroform exhibited three ^{31}P NMR signals coupled with ^{195}Pt at 88.2 ppm ($^1J_{\text{P-Pt}} = 2925$ Hz), 42.0 ppm ($^1J_{\text{P-Pt}} = 2492$ Hz) and 11.4 ppm ($^1J_{\text{P-Pt}} = 3675$ Hz), which can be assigned to the central and two terminal phosphorous atoms of the pp_3 ligand on a square-planar Pt(II) ion and the other terminal phosphorus atom bridging to another Pt(II) ion, respectively (Fig. 2). The NMR spectral simulation³ revealed a weak coupling ($^2J_{\text{P-P}} = 15$ Hz) between the two bridging phosphorus atoms (Fig. 3(a)) which are chemically equivalent⁴ and bound to the same Pt(II) ion. The

^{195}Pt NMR spectrum showed two signals: one is coupled with the two bridging phosphorus atoms ($^1J_{\text{Pt-P}} = 3675$ Hz) and the other is coupled with the central phosphorus atom ($^1J_{\text{Pt-P}} = 2920$ Hz) and the two terminal phosphorus atoms ($^1J_{\text{Pt-P}} = 2494$ Hz) (Fig. 4). These ^{31}P and ^{195}Pt NMR spectra confirmed the square-planar Pt(II)–Pt(II)–Pt(II) trinuclear structure.

Change in the ^{31}P NMR spectrum for the reaction solution of *trans*- $[\text{PtCl}_2(\text{NCC}_6\text{H}_5)_2]$ with **1** showed initial formation of the trinuclear complex different from **5** (Fig. 5), which was finally converted to **5** quantitatively in two days. A notable difference in the ^{31}P NMR spectra is the signal pattern for the central and bridging terminal phosphorus atoms, that is, the intermediate complex gives a relatively stronger coupling between the two bridging phosphorus atoms through the central Pt(II) ($^2J_{\text{P-P}} = 490$ Hz) compared with that of **5** (Fig. 3(b)). Such a difference in the coupling constants can be attributed to a difference in geometry around the central Pt(II) because similar values of $^2J_{\text{P-P}}$ (13 and 400 Hz) have been observed for the bridging phosphorus atoms in the *cis* and *trans* isomers of the Pd(II)–Pt(II)–Pd(II) heterotrinuclear complexes, respectively [8]. Consequently, the ^{31}P NMR spectral change indicates that the thermodynamically stabler *cis* isomer is finally formed by the isomerization on the Pt(II) center (Scheme 2). It should be emphasized here that predissociation of one of the terminal phosphino groups on **1** followed by attack onto the Pt(II) center of *trans*- $[\text{PtCl}_2(\text{NCC}_6\text{H}_5)_2]$ is required for the bridging reaction, considering the associative substitution mechanism of square-planar Pt(II) complexes [1].

³ gNMR version 5.0, Adept Scientific plc, Herts, UK, 2003.

⁴ The virtual $^2J_{\text{P-P}}$ coupling can be observed in the AA'XX' spin system, where A and A' and X and X' correspond to the two bridging and two central phosphorus atoms, respectively.

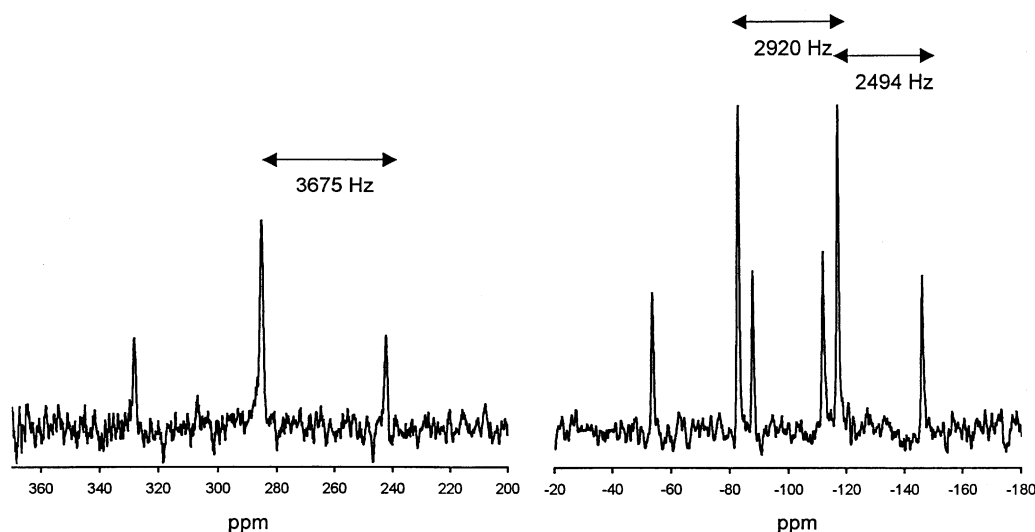


Fig. 4. ^{195}Pt NMR spectrum of **5** in CHCl_3 showing the $^1J_{\text{Pt-P}}$ values.

3.3. Substitution reaction

Because the substitution reaction of the pt complex **4** with halide ions did not proceed in completely dry conditions, the reactions of the chloro complex **1** with halide ions were examined. The ^{31}P NMR spectra of solutions containing vacuum-dried **1** and a large excess of $n\text{-Bu}_4\text{NX}$ ($\text{X}^- = \text{Br}^-$ and I^-) in dried chloroform changed to the spectra of **2** and **3**, respectively. The absorption spectra of the reaction solutions changed with isosbestic points at 448 and 312 nm for $\text{X}^- = \text{Br}^-$ and 438 and 340 nm for $\text{X}^- = \text{I}^-$ and finally agreed with those of **2** and **3**, respectively. The observed pseudo-first-order rate constants of the haro ligand substitution reactions (k_{obs})

were determined by nonlinear least-squares analyses for the exponential time courses of the absorbances at 340 nm for $\text{X}^- = \text{Br}^-$ and 360 nm for $\text{X}^- = \text{I}^-$.

As shown in Fig. 6, the observed rate constants at 298 K approach the respective limiting values as concentrations of the entering halide ions are increased. Because formation of an intermediate with a dissociated terminal phosphino group is probable considering the rapid equilibrium and the oxidation reaction of **4** and the bridging reaction of **1** (vide supra), two reaction mechanisms can be expected for such a saturation behavior: one is the limiting dissociative mechanism in which the unstable four-coordinate square-planar intermediate is generated by the predissociation of one of the

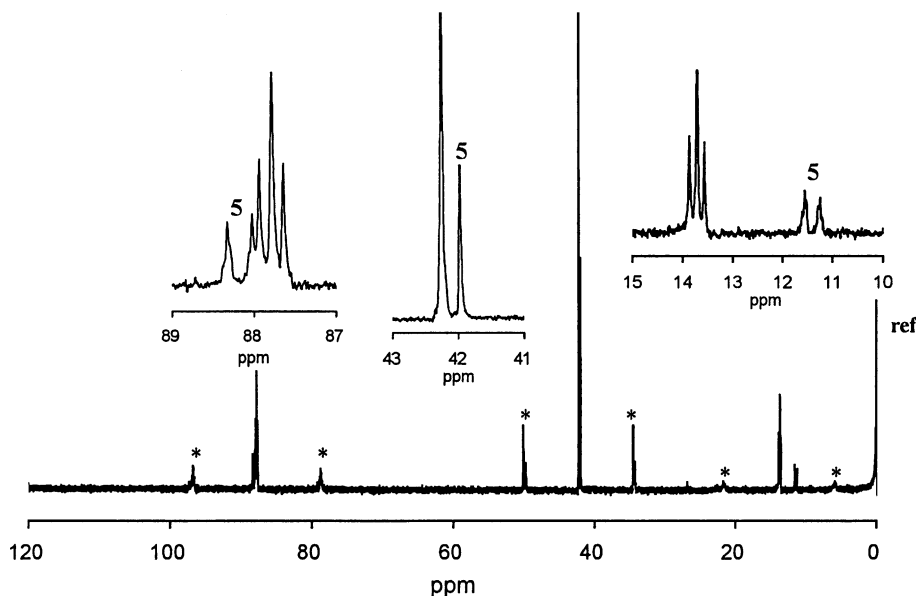
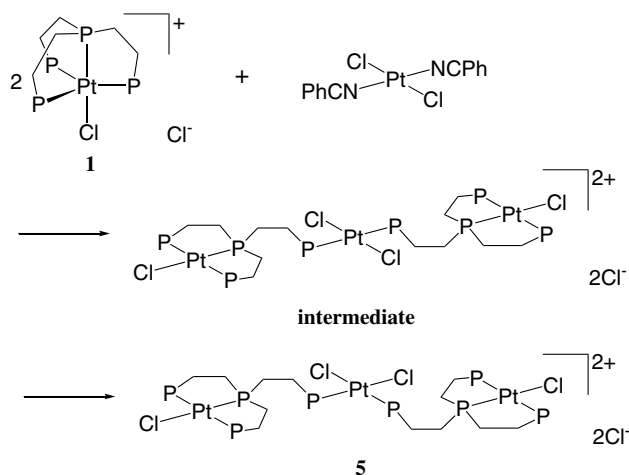


Fig. 5. ^{31}P NMR spectrum for the solution containing **1** ($3.0 \times 10^{-2} \text{ mol kg}^{-1}$) and $\text{trans-[PtCl}_2(\text{NCC}_6\text{H}_5)_2]$ ($1.5 \times 10^{-2} \text{ mol kg}^{-1}$) in chloroform at 45 min after preparation. **5s** denote the signals for the corresponding complex. Asterisks and 'ref' denote satellite peaks due to ^{195}Pt and the signal for D_3PO_4 in the outer D_2O , respectively.



Scheme 2. Formation reaction of 5.

terminal phosphino groups (Mechanism I in Scheme 3) and the other is the preassociation mechanism in which the square-pyramidal intermediate similar to **1** detected for **4** is present in rapid pre-equilibrium (Mechanism II in Scheme 3). The limiting value of k_{obs} obtained by a least-squares analysis for $X^- = \text{Br}^-$ is about several times that for $X^- = \text{I}^-$. Because the limiting values of k_{obs} in Mechanism I are equal to the predissociation rate constant k_1 that is independent of the entering halide ions, Mechanism II via the preassociation intermediate with a dissociated terminal phosphino group and an apically coordinated halide ion is reasonably expected. The values of the pre-equilibrium constant (K) and the successive dissociation rate constant (k) for each entering

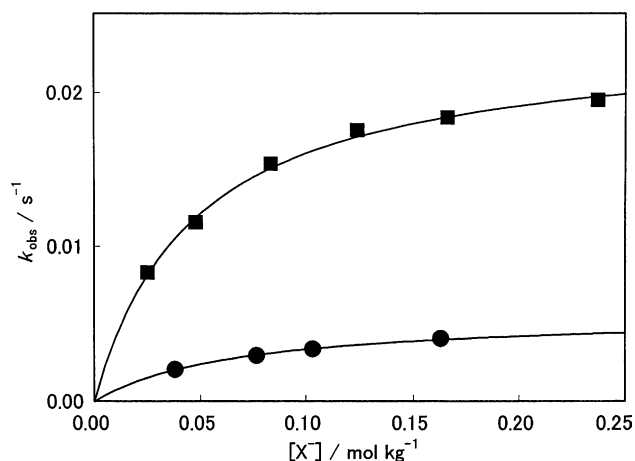


Fig. 6. Dependence of the observed rate constants for the chloro-ligand substitution reactions of **1** in chloroform at 298 K on the concentrations of the entering Br^- (●) and I^- (■). The solid lines were depicted by using the equation for Mechanism II and the corresponding K and k values in Table 1.

halide ion were obtained by a least-squares analysis according to the equation: $k_{\text{obs}} = Kk[X^-]/(K[X^-] + 1)$ (Table 1). Assuming that the equilibrium constants for the trigonal-bipyramidal–square-pyramidal geometrical change of the halo complexes **1–3** are comparable to the pre-equilibrium constants obtained kinetically here, concentrations of the square-pyramidal species for **1–3** are quite low under the concentration conditions for the NMR and absorption spectral measurements in the present work. The latter dissociation step probably proceeds by a reaction mechanism similar to that for general square-planar Pt(II) and Pd(II) complexes in

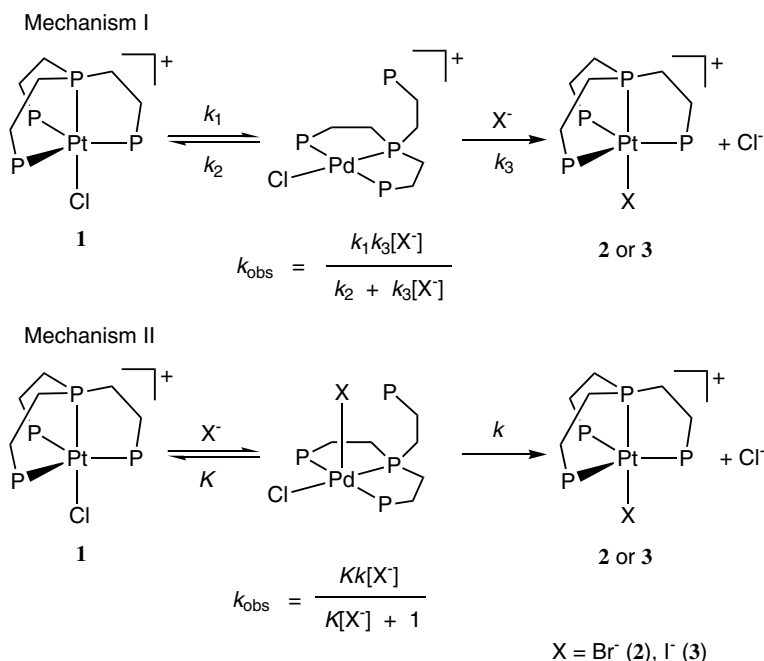
Scheme 3. Possible mechanisms for the substitution reactions of **1**.

Table 1

Pre-equilibrium constants (K) and dissociation rate constants (k) for the substitution reactions of **1** with Bu_4NX ($\text{X}^- = \text{Br}^-, \text{I}^-$) in chloroform at 298 K.

| X^- | K^{298} ($\text{mol}^{-1} \text{kg}$) | k^{298} (s^{-1}) |
|---------------|---|----------------------------------|
| Br^- | $(1.53 \pm 0.05) \times 10^1$ | $(5.48 \pm 0.10) \times 10^{-3}$ |
| I^- | $(2.02 \pm 0.04) \times 10^1$ | $(2.40 \pm 0.08) \times 10^{-2}$ |

which the entering ligand X^- shifts to the square-plane and pushes away the leaving chloro ligand via the trigonal-bipyramidal transition state. Accordingly, the apparently greater rate constant k for $\text{X}^- = \text{I}^-$ is attributed to the π -accepting ability of the iodo ligand, which can stabilize the transition state with the entering X^- and leaving chloro ligands and the central phosphorus atom in the trigonal plane. In the case of the present pp_3 complexes, the substitution reactions are completed by the chelate-ring closure of the dissociated terminal phosphino group.

In general, the equatorial phosphorus atoms are weakly coordinated to d^8 metal ions compared with the axial one for the trigonal-bipyramidal pp_3 complexes [2,4e,5]. Furthermore, it should be mentioned here that the average equatorial Pd–P distance for $[\text{PdCl}(\text{pp}_3)]\text{Cl}$ (2.432 Å) [2] is definitely longer than the corresponding Pt–P distances for $\mathbf{1} \cdot \text{CH}_3\text{CN}$ (2.375 Å) and $\mathbf{1} \cdot 6\text{H}_2\text{O}$ (2.369 Å) [5], while the axial Pt–P distances are comparable (2.221–2.237 Å) [2,5]. These facts leave place for argument that the substitution reactions of the trigonal-bipyramidal Pd(II) complexes with the pp_3 ligand also proceed via similar intermediates with a dissociated terminal phosphino group.

4. Supplementary material

^{31}P NMR spectra of $[\text{Pt}(\text{pt})(\text{pp}_3\text{O})](\text{BF}_4)$ (Fig. S1) and the reaction solution containing **4** and $N\text{-Bu}_4\text{NI}$ (Fig. S2) in chloroform, detailed thermodynamic and kinetic data for the reactions of **4** with I^- in chloroform (Fig. S3 and S4, respectively) and crystallographic data of $\mathbf{1} \cdot \text{H}_2\text{O}$ in CIF format are available from the author upon request.

5. Acknowledgments

This work was supported by a grant from Kurita Water and Environment Foundation and Grant-in-Aid for Scientific Research (No. 15550104) from the Ministry of Education, Culture, Sports, Science and Technology of Japan.

References

- [1] (a) R.G. Wilkins, *Kinetics and mechanism of reaction of transition metal complexes*, second ed., VCH, Weinheim, 1991 (Chapter 4); (b) R.J. Cross, M.V. Twigg, *Mechanisms of Inorganic and Organometallic Reactions*, Plenum Press, New York, 1988 (Chapter 5); (c) Z. Lin, M.B. Hall, *Inorg. Chem.* 30 (1991) 646.
- [2] S. Aizawa, T. Iida, S. Funahashi, *Inorg. Chem.* 35 (1996) 5163.
- [3] S. Aizawa, T. Iida, Y. Sone, T. Kawamoto, S. Funahashi, S. Yamada, M. Nakamura, *Bull. Chem. Soc. Jpn.* 75 (2002) 91.
- [4] (a) R.B. King, R.N. Kapoor, M.S. Saran, P.N. Kapoor, *Inorg. Chem.* 10 (1971) 1851; (b) C.A. Ghilardi, S. Midollini, L. Sacconi, *Inorg. Chem.* 14 (1975) 1790; (c) A. Orlandini, L. Sacconi, *Inorg. Chem.* 15 (1976) 78; (d) L. Sacconi, P. Dapporto, P. Stoppioni, P. Innocenti, C. Benelli, *Inorg. Chem.* 16 (1977) 1669; (e) W.H. Hohman, D.J. Kountz, D.W. Meek, *Inorg. Chem.* 25 (1986) 616; (f) P. Brüggeller, *Inorg. Chem. Acta* 129 (1987) 27; (g) C. Bianchini, A. Meli, M. Peruzzini, F. Zanobini, *Organometallics* 9 (1990) 241; (h) C. Bianchini, A. Meli, M. Peruzzini, F. Vizza, *Organometallics* 9 (1990) 1146; (i) C. Bianchini, P. Innocenti, A. Meli, M. Peruzzini, F. Zanobini, *Organometallics* 9 (1990) 2514; (j) M.C. Vaira, M. Peruzzini, P. Stoppioni, *Inorg. Chem.* 30 (1991) 1001.
- [5] D. Fernández, M.I.G. Seijo, T. Kégl, G. Petőcz, L. Kollár, M.E.G. Fernández, *Inorg. Chem.* 41 (2002) 4435.
- [6] A.B.P. Lever, *Inorganic Electronic Spectroscopy*, second ed., Elsevier, Amsterdam, 1984 (Chapter 6).
- [7] (a) U. Belluco, R. Ettorre, F. Basolo, R.G. Pearson, A. Turco, *Inorg. Chem.* 5 (1996) 591; (b) J.R. Paxson, D.S. Martin Jr., *Inorg. Chem.* 10 (1971) 1551; (c) L. Helm, L.I. Elding, A.E. Merbach, *Helv. Chim. Acta* 67 (1984) 1453.
- [8] S. Aizawa, T. Kawamoto, K. Saito, *Chem. Lett.*, to be submitted.